Full Title: Highly sensitive *in vivo* detection of dynamic changes in enkephalins following acute stress

Short Title: *In vivo* detection of enkephalins during stress

Authors: Marwa O. Mikati[1,2,3], Petra Erdmann-Gilmore[4], Rose Connors[4], Sineadh M. Conway[1,2,3], Jim Malone[4], Justin Woods[1,2,3], Robert W. Sprung[4], R. Reid Townsend[4], Ream Al-Hasani* [1,2,3].

[1]Department of Anesthesiology, [2]Washington University Pain Center, Washington University in St. Louis, MO, USA; [3]Center for Clinical Pharmacology, University of Health Science and Pharmacy in St. Louis, MO, USA, [4]Department of Medicine, Washington University School of Medicine, Washington University in St. Louis, St. Louis, MO, USA

***Correspondence:** Ream Al-Hasani, PhD: al-hasanir@wustl.edu.

Abstract: Enkephalins are opioid peptides that modulate analgesia, reward, and stress. *In vivo* detection of enkephalins remains difficult due to transient and low endogenous concentrations and inherent sequence similarity. We present an analytical method for Met- and Leu-Enkephalin (Met-Enk & Leu-Enk) detection in the mouse Nucleus Accumbens shell (NAcSh) after acute stress. We confirm that acute stress activates enkephalinergic neurons in the NAcSh using fiber photometry and that this leads to the release of Met- and Leu-Enk. We also demonstrate the dynamics of Met- and Leu-Enk release as well as how they correlate to one another in the ventral NAc shell, which was previously difficult due to the use of approaches that relied on mRNA transcript levels rather than post-translational products. This approach increases spatiotemporal resolution, optimizes the detection of Met-Enkephalin through methionine oxidation, and provides novel insight into the relationship between Met- and Leu-Enkephalin following stress.

Teaser: An improved method for measuring opioid peptides *in vivo* demonstrates their role in acute stress.

Introduction

Endogenous opioid peptides are released at significantly lower concentrations than small molecule neurotransmitters and undergo post-translational processing that yields ~30 unique peptides from 4 precursor molecules. Together, these properties have made sensitive peptide detection difficult to achieve with existing technologies [1]. Here, we describe an analytical method that enables quantification of dynamic *in vivo* changes in both Leu- and Met-enkephalin (Leu-Enk and Met-Enk) peptides in rodents. We show unique release profiles between Leu- and Met-Enk in response to two different stressors and gain new insight into peptide release dynamics; additionally, our method offers improved spatiotemporal resolution. More broadly, this approach will enable an understanding of how neuropeptide levels change in response to acute or chronic behavioral, pharmacological, and neurophysiological manipulations.

Enkephalins can act on both the delta and/or mu opioid receptors, but their activity often depends on receptor and peptide expression patterns, which differ across the brain [2–5]. Confirming an opioid peptide's identity based on the activity of the receptor alone poses difficulties. For example, in a single brain region, the mu opioid receptor may be activated by an enkephalin or endorphin peptide [3]. Therefore, any technique that relies on a readout of mu opioid receptor activity is not sufficient to determine whether the peptide is an endorphin or an enkephalin. It has been particularly challenging to measure Met- and Leu-Enk selectively and independently *in vivo*; in fact, both peptides are typically referred to as 'enkephalins', which oversimplifies their distinct properties. Though antibody-based techniques [6–8] or liquid chromatography/mass spectrometry (LC-MS) [9–12] have improved Met- and Leu-Enk detection somewhat, limitations such as spatiotemporal restrictions and poor selectivity between enkephalins remain. Our group previously developed real time *in vivo* detection of evoked opioid peptide release using microdialysis/nanoLC-MS (nLC-MS) after photostimulation [13]. From this strong foundation, we have now optimized a novel opioid peptide detection technique. For the first time, we can selectively measure real-time *in vivo* levels of basal (non-evoked) peptide release as well as during behavioral manipulations. Our primary goals in establishing this analytical workflow to measure opioid peptide dynamics *in vivo* were to 1) increase temporal resolution allowing for the detection of dynamic changes to short external stimuli and acute conditions, 2) lower the detection threshold to allow for accurate measurements from small brain regions using less volume of sample, 3) measure endogenous release of peptides in the native state without the need for photo- or chemogenetic stimulation, 4) report raw values of measured concentrations rather than % baseline measurements. To meet these goals and measure both Leu- and Met-Enk we used an improved and specialized microdialysis technique coupled with nLC-MS.

Results

Optimizing a method for the simultaneous *in vivo* detection of Met- and Leu-Enkephalin

68 Our workflow (**Fig. 1A**) starts with stereotaxic surgery to implant the microdialysis probe in the
69 mouse nucleus accumbens shell (NAcSh). Along with others, we have shown that the opioid
70 receptor system in the NAcSh mediates both reward and aversion through photostimulation of
71 peptide-expressing neurons across the dorsal/ventral axis [14–20]. Our aim was to measure
72 NAcSh peptide release in response to aversive, stressful stimuli. We use custom-made
73 microdialysis probes, intentionally modified so they are similar in size to commonly used fiber
74 photometry probes to avoid extensive tissue damage caused by traditional microdialysis probes
75 (**Fig. 1B**). Importantly, the membrane that sits above the brain region of interest is smaller in
76 diameter when compared to a photometry probe (**Fig. 1B**). After recovery, we begin microdialysis
77 collection every 13 minutes, circulating artificial cerebrospinal fluid (aCSF) and collecting
78 interstitial fluid (ISF) at a flow rate of 0.8 μL/min. After each sample collection, we add a consistent
79 known concentration of isotopically labeled internal standard of Met-Enk and Leu-Enk to the
80 collected ISF for the accurate identification and quantification of endogenous peptide. These
81 internal standards have a different mass/charge (m/z) ratio than endogenous Met- and Leu-Enk.
82 Thus, we can identify true endogenous signal for Met-Enk and Leu-Enk (**Suppl Fig. 1A,C**) versus
83 noise and interfering signals (**Suppl. Fig. 1B,D**). Importantly, we have resolved one of the main
84 barriers preventing the accurate quantification of Met-Enk: the variable oxidation of the methionine
85 residue during sample processing, which results in the signal for Met-Enk being split among
86 multiple m/z values thereby impairing sensitivity. In order to ensure that the signal for Met-Enk is
87 represented by a single m/z value, we converted all methionyl residues to the doubly oxidized
88 sulfone prior to nLC-MS analysis, which allows us to reliably quantify Met-Enk and differentiate it
89 from Leu-Enk [21]. Beyond opioid peptides, this approach represents a key advance and can be
90 applied to any peptide containing a methionine residue. As seen in **Fig. 1C.**, before the methionine
91 oxidation reaction at time 0, Met-Enk can be observed in unoxidized, and singly- and doubly-
92 oxidized forms with varying intensities. However, after the reaction is complete at time 1, Met-Enk
93 is observed as doubly oxidized with much higher intensity enabling accurate quantification.

To increase the signal to noise ratio, we also performed solid-phase extraction after the oxidation reaction which removes any salt from the collected samples. To determine the lower limit of quantification (LLOQ), forward and reverse curves were created using varying concentrations of the Met- and Leu-Enk standards in accordance with Clinical Proteomics Tumor Analysis Consortium (CPTAC) guidelines [22]. We determined that the lower limit of quantification (LLOQ), for both Leu-Enk and Met-Enk is 40 amol/sample (**Fig. 1D-E**). The improved quantification limit means increased temporal resolution. We now need less volume, (10 μL or less), and shorter sampling times: 10 minutes or less, rather than 15-20 minutes as compared to previous studies [13,23]. To test the utility of the method in measuring real-time changes in peptide levels *in vivo*, we evoked the release of the peptides using high K^+ ringer's solution, which depolarizes the cells and causes the release of dense core vesicles containing neuropeptides [24]. This depolarization state significantly increased the release of Met- and Leu-Enk in the NAcSh as compared to baseline **Fig.1F**. Previous studies reporting opioid peptide measurements rarely represent raw concentrations measured. Instead, most past studies reported changes in peptide concentrations as % of baseline [10,13,23]. One key advantage of our improved method is that we can detect reliable measurements of both Met- and Leu-Enk at baseline that we can report concentrations in the amol/sample range. We then quantified the ratio of the Met- to Leu-Enk after applying high K+ solution and showed that this ratio is 3:1 in the NAcSh (**Fig. 1G-H**). The release of Met-Enk is postulated both in vitro and ex vivo to be between 3 to 4 times that of Leu-Enk [25–27]. We are the first to not only corroborate the predicted ratio *in vivo,* but specifically in the NAcSh. Interestingly, this 3:1 ratio is almost identical to that previously reported in homogenized human tissue from the sympathoadrenal systems using radioimmunoassays [28]. Importantly, this conserved ratio highlights the usefulness of rodent models for investigating the highly conserved opioid system and demonstrates its potential in translation to humans.

120 **Experimenter handling drives the release of Met- and Leu-Enkephalins in the NAcSh**

121 To highlight the applicability and value of this improved approach, we investigated the changes
122 in the levels of enkephalins following acute stress. It has been hypothesized that enkephalins act
123 as anti-stress signals based on studies that have shown increased preproenkephalin transcript
124 levels following acute stress [29–32]. Moreover, decreased enkephalin expression in the NAc was
125 correlated with an increase in the susceptibility to social defeat [33]. Our group has also recently
126 demonstrated that the photostimulation of a subpopulation of peptidergic neurons in the NAcSh
127 drives aversion [14], which further suggests a role for neurons in the NAcSh during aversive
128 stimuli such as stress. Despite the wealth of data implicating these peptides in the stress
129 response, it has not been possible to measure the dynamics of real-time peptide release in
130 response to acute stressful stimuli. We sought to test the hypothesis that Met- and Leu-Enk are
131 released in the NAcSh following acute stress. Using the nLC-MS detection method, we
132 successfully monitored dynamic changes of Met- and Leu-Enk during two different stressors. The
133 first stressor was defined as experimenter handling, which involves the experimenter scruffing the
134 mouse while connecting to the dialysis set up (**Fig. 1A**). The second stressor was exposure to
135 predator odor (i.e., fox urine).

136

137 We show that both Met- and Leu-Enk are released following experimenter handling, and that the
138 levels decrease within minutes after exposure to the stress (**Fig. 2A**). We also analyzed the data
139 with sex as a main effect and did not find any differences between males and females after
140 correcting for multiple comparisons (**suppl. Fig. 2A**). We corroborate our finding from **Fig. 1G-H**
141 showing that the ratio of 3:1 Met-Enk to Leu-Enk is conserved following experimenter handling
142 (**Fig. 2C**). Another key finding is that peptide release appears to be precisely controlled. We show
143 that the amol/sample of Met-Enk released at the beginning of the experiment is predictive of later
144 release. For example, a higher level released (in the fmol/sample range) during the first collections
145 results in lower levels released (in the amol/sample range) during later collections and vice versa

146 (**Fig. 2D**). We show a negative correlation (~ -0.3) between the first two samples (~26 minutes)
147 and the later timepoints, samples 3-10 (~104 minutes). Importantly, this relationship is not due to
148 Met-Enk depletion as the circulation of high K+ aCSF is sufficient to drive the release of Met-Enk
149 at the end of an experiment and reverse the negative correlation (**Fig. 2E**).
150
151 To test whether our findings regarding peptide release correlated with neuronal activity following
152 the same stressor, we also monitored enkephalinergic neuron activity using fiber photometry
153 following experimenter handling. To do this, we stereotaxically injected a Cre-dependent adeno-
154 associated virus containing the calcium sensor GCaMP6s in the NAcSh of preproEnkephalin-Cre
155 (pEnk-Cre) mice and implanted fiber photometry probes (**Fig. 2F**). During handling, we observed
156 increased calcium activity in enkephalinergic neurons, even after it was repeated twice within a
157 few minutes (**Fig. 2G**). Individual responses to experimenter handling varied appreciably, as
158 shown by the heatmaps and bar plots (**Fig. 2H-I**); such variation could be due to slight differences
159 in probe placement (**Suppl. Fig 3B,D**) as peptidergic neurons in the dNAcSh encode reward while
160 neurons in the vNAcSh encode aversion [14,34]. Furthermore, the enkephalin precursor is
161 expressed across the dorsal-ventral axis as shown in the *in situ* hybridization atlas (Allen Brain
162 Institute). The fiber photometry data and peptide release data are concordant, as enkephalinergic
163 neurons are activated following experimenter handling, which drives Met- and Leu-Enk
164 somatodendritic release. However, the photometry and peptide release data differ in that repeated
165 neuronal activation may not necessarily lead to repeated peptide release, as suggested by the
166 decrease in peptide release over time in **Fig. 2D**. Additionally, fiber photometry cannot provide
167 information about Met- and Leu-Enk independently, as it relies on the precursor gene, *penk*.
168 Taken together, our data highlight the value and importance of coupling fiber photometry results
169 with in vivo measurements of neuropeptides to determine release dynamics.
170
171

172 **Predator odor causes the release of Met-Enkephalin in the Nucleus Accumbens Shell**

173 We wanted to test another stressor that is similar in nature to experimenter handling as the
174 experimenter represents aversive visual, olfactory, and touch stimuli to the mouse. Fox odor has
175 been widely demonstrated to be aversive to rodents and other mammalian species [35–37]. The
176 benefit of using predator odor is that it represents what mice would encounter in the wild, outside
177 of the lab environment. It also allows us to probe conserved circuits in laboratory mice related to
178 aversion, threat, and defensive behaviors. Prior reports have shown that predator odor leads to
179 an increase in the expression of the neuronal activation-associated transcription factor fos in
180 enkephalin-positive neurons in different brain regions including the NAcSh [38,39]. Therefore, we
181 sought to determine whether enkephalins are released in the NAcSh following exposure to fox
182 urine. We first measured calcium activity of enkephalinergic neurons using fiber photometry after
183 exposure to fox urine (**Fig. 3A**). We show that upon first exposure, the activity of enkephalinergic
184 neurons is markedly increased (**Fig. 3B-D**). However, this enkephalinergic activity is significantly
185 attenuated during second and third exposures that are separated by five minutes suggesting
186 habituation to the stimulus (**Fig. 3B-D**). To determine whether the response to fox urine may also
187 be due to the novelty of the weigh boat used to introduce the fox urine, we measured
188 enkephalinergic calcium activity after introducing a weigh boat containing water to the home cage
189 (**Suppl. Fig. 4A**). Interestingly, we show that enkephalinergic neurons also respond to the
190 introduction of a novel object, and the response to the water-containing weigh boat is attenuated
191 upon repeated exposure, which is what we observed for fox urine (**Suppl. Fig. 4B-D**). We
192 compared the enkephalinergic neuron activation in response to both water and fox urine for each
193 individual mouse that experienced both, and we see similar calcium transient responses to both
194 the introduction of a novel object and the odor of a predator, suggesting the same subpopulation
195 of enkephalinergic neurons may have been activated (**Suppl Fig. 4E**). Interestingly and
196 importantly, only recently have researchers shown that a higher level of spiking in the striatum is
197 not always reflected in greater photometry transients [40]. In the future, it will be important to

198 determine whether the fox urine response indeed shows higher action potential spiking than the
199 weigh boat with water. Although the calcium responses to both the fox-urine and water-containing
200 weigh boats were similar in magnitude, it may be that different subpopulations of enkephalinergic
201 neurons are activated in the NAcSh. Further exploration of the specific neurons that respond to
202 the introduction of a novel object or the odor of a predator is warranted. We concluded that
203 enkephalinergic neurons are activated by fox odor using fiber photometry. We were then
204 interested in testing whether activation of enkephalinergic neurons leads to release of Met- and
205 Leu-Enk, so we measured peptide levels in the NAcSh after fox odor using our method of
206 microdialysis and nLC-MS (**Fig. 3E**).
207
208 In this separate group of animals, we show that there is a significant increase in Met-Enk release
209 after exposure to fox odor (**Fig. 3F**). The response to predator odor varies appreciably: although
210 most animals show increased Met-Enk release after fox odor exposure, some show continued
211 release with no elevation in Met-Enk levels, and a minority show no detectable release (**Fig. 3G**).
212 Enkephalins are thought to mediate resilience to stress, so the individual differences in responses
213 to predator odor may indicate differences in stress adaptability [32,41–43]. Moreover, no sex
214 differences in the responses to fox urine were observed, similar to responses to experimenter
215 handling (**Suppl. Fig. 2B**). It is also worth noting that we only observed Leu-Enk release in 3 of
216 16 experiments. This is likely due to Leu-Enk not being released following predator odor or
217 because it is released at a level below the LLOQ, as suggested by the observed 3:1 ratio of Met-
218 Enk to Leu-Enk (**Fig. 3G**).
219
220 **Discussion**
221 In summary, this work allows for multiple unique advances in studying endogenous opioids and
222 neuropeptides in general. Although there has been substantial progress in fluorescent sensor-
223 based techniques, electrochemical approaches, and immunoaffinity based assays, the

224 investigation of opioid peptides has lagged due to their unique properties: sequence similarity,
225 diversity, and low concentrations. Here, we address these challenges by advancing microdialysis
226 coupled with nLC-MS. First, we have developed a method of methionine stabilization that is
227 transferrable to other neuropeptides and have decreased the LLOQ and temporal resolution,
228 which are typically the main critiques of microdialysis and LC-MS approaches. As we have shown,
229 if Met-Enk is not fully oxidized prior to LC-MS analysis, it is hard to quantify because of the
230 presence of differentially oxidized species. The diversity of the signal detected impedes the
231 analysis of a single sample and may lead to inaccurate concentration values. Second, we
232 quantified the relationship between Leu- and Met-Enk and offer a definitive *in vivo* ratio (3:1 Met-
233 Enk to Leu-Enk) that has long been in question; this ratio corroborates human data [28] and
234 suggests that mice are a useful model system for the study of enkephalinergic release dynamics.
235 Based on this, future studies investigating the use of opioid peptides as biomarkers for psychiatric
236 conditions will be readily translatable from rodents to humans and will allow for ease in reverse
237 translation efforts. There is already some demonstrated interest in measuring opioid peptide
238 levels in humans due to their roles in mood disorders, substance use, and pain [44,45]. Moreover,
239 prior to our study, the predicted ratio of Met- to Leu-Enk was predicted based on the mRNA
240 transcript sequence, so we are the first to confirm that post-translational cleavage indeed yields
241 the predicted ratio. Third, we identify a role for the NAcSh in the acute stress response by
242 demonstrating local release of Met- and Leu-Enk after stress exposure using our improved
243 microdialysis and nLC-MS method. Although studies have suggested a role for the NAcSh in
244 stress through measurements of *penk* transcripts, it had not been definitively shown that there is
245 local release of enkephalins after stress exposure [33,46]. We also expanded our findings by
246 showing that enkephalinergic neurons are activated by stress exposure, both experimenter
247 handling and fox odor, using fiber photometry. Repeated experimenter handling led to repeated
248 activation of enkephalinergic neurons. However, fox odor exposure showed significant
249 attenuation after the first exposure. This is consistent with prior studies showing fast habituation

250 to olfactory stimuli in rodents after initial exposure [35–37,47]. We also showed using fiber
251 photometry that the novelty of the introduction of a foreign object to the cage, before adding fox
252 odor, was sufficient to activate enkephalinergic neurons. This is consistent with the object being
253 a stressor as it is newly introduced to the homecage. Alternatively, it could also mean that the
254 stress response is more nuanced and is impacted by the novelty of the stressor. This is an area
255 of interest to our group, and we will design future experiments to disentangle the novelty from the
256 stressor in order to understand the enkephalinergic system better. Given that previous studies
257 implicating enkephalins in stress used mRNA transcript measurements of proenkephalin, it was
258 not possible to determine whether Leu- and/or Met-Enk were involved in the acute stress
259 response. Our study suggests that both peptides are involved in experimenter handling stress,
260 while fox odor may or may not cause Leu-Enk release. Most of our experiments with fox odor
261 showed no Leu-Enk release, however, that could be due to Leu-Enk levels being below the LLOQ
262 since we have demonstrated that it is 3 times lower than Met-Enk. Fourth, we show that Met- and
263 Leu-Enk are released during acute stress in the NAcSh, offering evidence for their role in gating
264 the stress response which was suggested based on studies of enkephalins in the Locus
265 Coeruleus [32]. Therefore, combined with other studies, our work suggests that the role of
266 enkephalins in stress is generalizable to other brain regions, namely the ventral striatum. Based
267 on our findings, it remains unclear how enkephalins modulate the stress response. It will be
268 interesting to investigate whether enkephalinergic signaling modulates stress coping behaviors.
269 Future studies will focus on determining the effect of the local release of Met- and Leu-Enk in the
270 NAcSh on responses to stress in rodents. Finally, when a limited amount of peptide is released
271 over time, we show that peptide release is biologically constrained and can be experimentally
272 driven using high K+ buffer or photo or chemogenetic stimulation [13]. We also show that data
273 from fiber photometry corroborate peptide release data; however, fiber photometry does not offer
274 the necessary specificity to correlate activation with release, or the distinction between different
275 peptides that arise from the same precursor molecule. Additionally, it is important to stress that

276 our fiber photometry studies used a calcium sensor as a proxy for neuronal activity and the
277 temporal scale was on the order of seconds. A recent study using an opioid-peptide fluorescent
278 sensor shows temporal scales on the order of minutes, which mirrors microdialysis timelines for
279 neuropeptide detection, and offers evidence that neuropeptide dynamics are generally much
280 slower than neurotransmitters *in vivo* [48]. In conclusion, this improved peptide detection method
281 enables biological advances through an optimized approach for Met- and Leu-Enk detection *in*
282 *vivo* with broad applicability to other neuropeptides.

Figures and Legends:

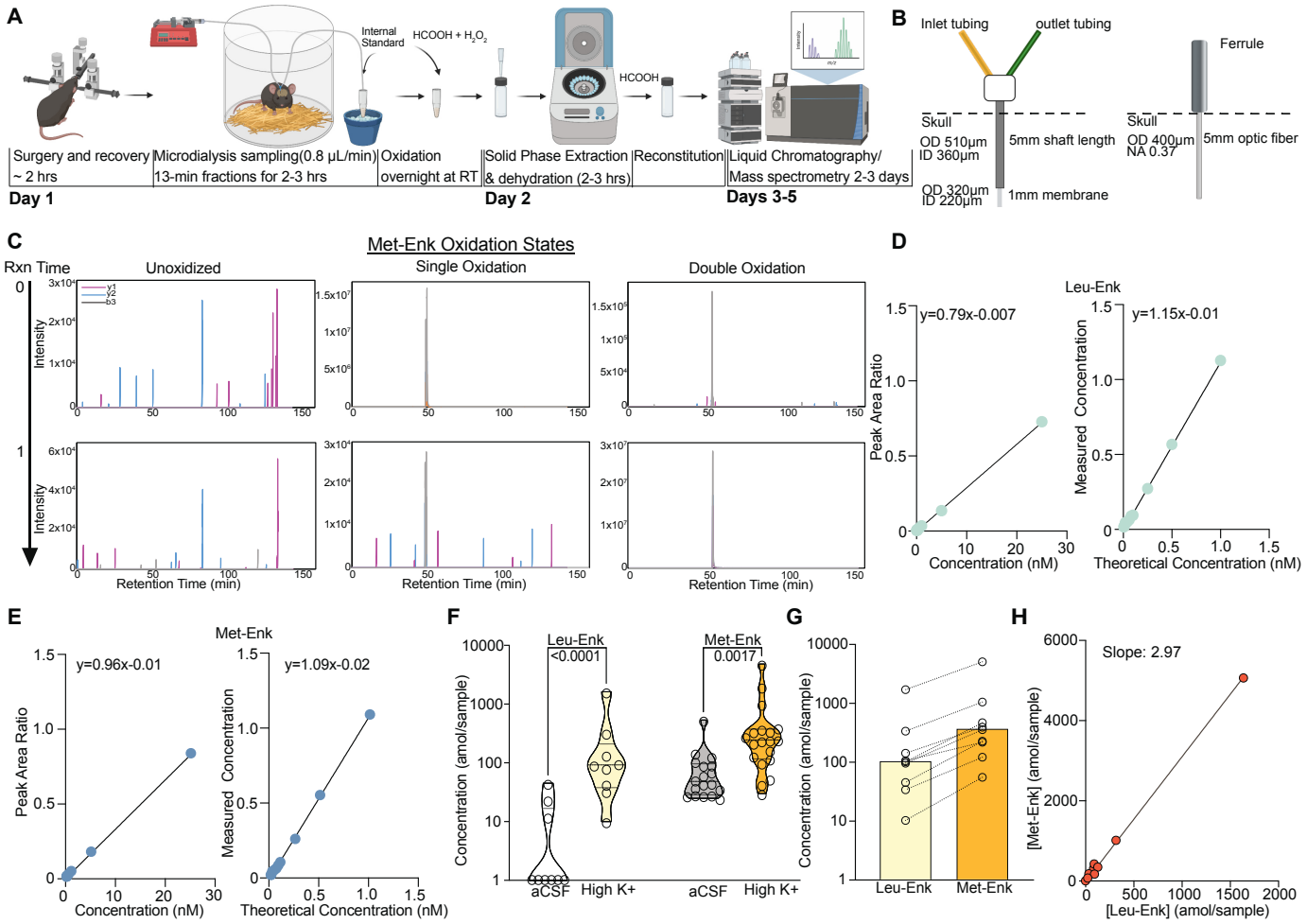

Figure 1: An optimized approach for *in vivo* Met- and Leu-Enk measurement. **A.** Timeline of *in vivo* sample collection on day 1 and methionine oxidation reaction overnight, sample processing on day 2, and data acquisition on the LC-MS, days 3-5. The microdialysis probe is implanted via stereotaxic surgery in the Nucleus Accumbens Shell. The mouse is allowed to recover before being connected to the microdialysis lines. Samples are then collected at a rate of 0.8 μL/min for 13 minutes each. After collection is completed, the samples are oxidized overnight. On day 2 the samples undergo solid phase extraction (SPE) and are then dehydrated and reconstituted using formic acid (HCOOH) before being acquired on the LC-MS. **B**. Custom microdialysis probe specifications including membrane size and inner and outer diameters (ID and OD respectively) compared to fiber photometry probe specifications including OD of optic fiber and numerical aperture (NA). **C**. Before the methionine oxidation at reaction (Rxn) time 0, Met-Enk exists in three different forms with varying intensities, unoxidized (multi-peak), singly oxidized (multi-peak), and doubly oxidized (single peak). After the reaction completes (Rxn time 1), most of the detected signal is in the doubly oxidized form and shows a single peak (>99% signal intensity). **D.** (Left) Forward calibration curve of Leu-Enk and Met-Enk showing the peak area ratios as the light standard levels are varied. **(**Right**)** Reverse calibration curve of Leu-Enk showing the relationship between the heavy standard concentration applied and the measured concentration based on the instrument. **E.** Same setup as **D** but for Met-Enk**. F.** Violin plots showing that high K+ ringer's solution increases the release of both Leu-Enk and Met-Enk compared to baseline levels in artificial cerebrospinal fluid (aCSF) (Leu-Enk n=9, Met-Enk n=18). The dashed center line indicates the median. **G.** The evoked concentrations of Met-Enk to Leu-Enk in the same samples show that Met-Enk is consistently released at a higher level than Leu-Enk (n=9). **H.** Met-Enk is released at a factor of 2.97 that of Leu-Enk as shown by linear regression analysis of the data in f, suggesting a linear relationship between the two peptides. Data in **F**, **G**, and **H** are transformed to a log scale. In **F**, 2-way ANOVA analysis shows a main effect of peptide, solution, and interaction. The *p*-values reported were calculated using a Sidak's multiple comparisons test.

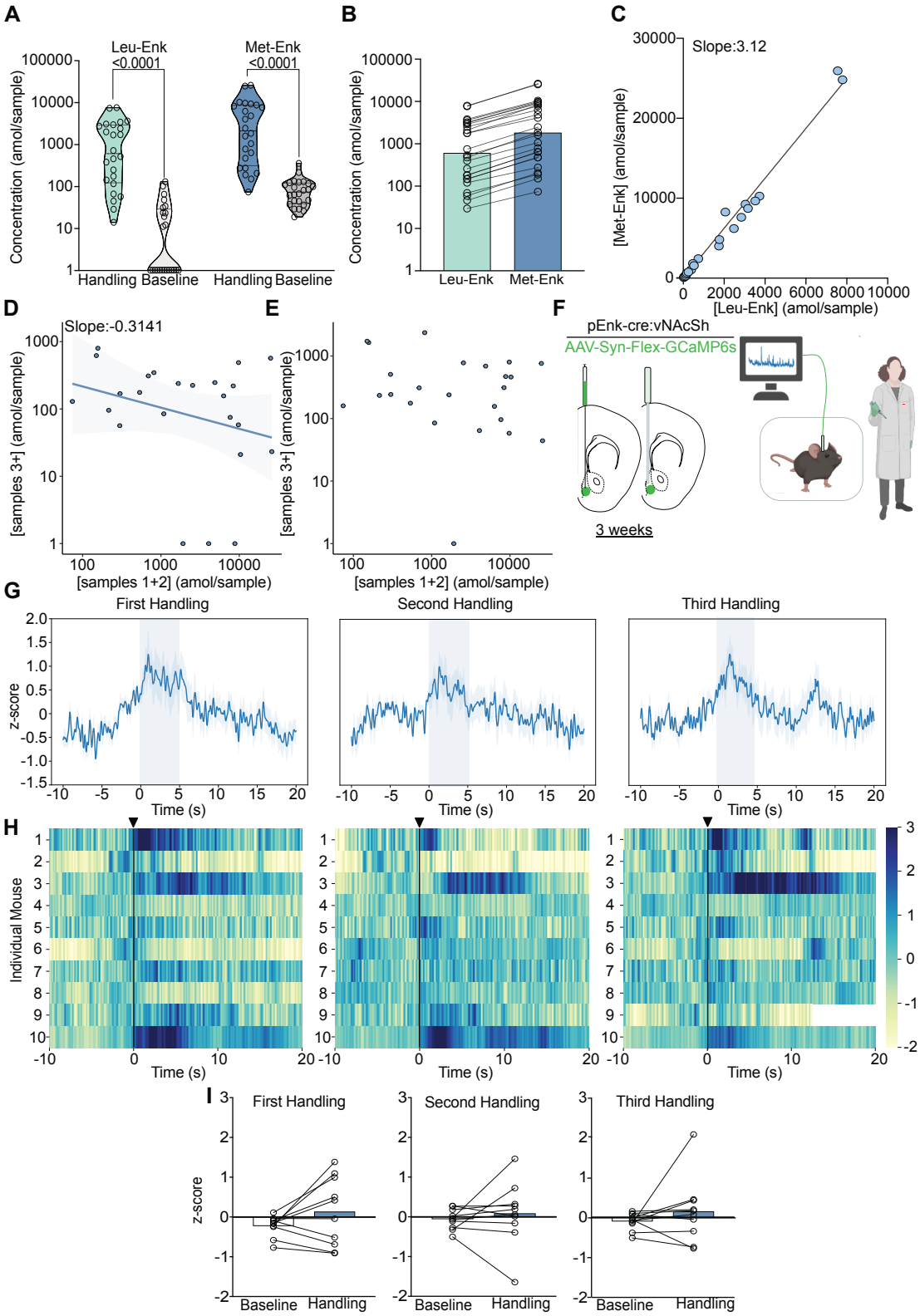

314
315
316
317

Figure 2: Experimenter handling evokes the release of Met- and Leu-Enk in the NAcSh. A. Experimenter handling during microdialysis causes a significant increase in the release of Leu- and Met-Enk in comparison to baseline. **B.** During experimenter handling, Met-Enk is consistently released at a higher rate than Leu-Enk in the same samples. **C.** Linear regression analysis of the data in **B** shows that Met-enk is released at a rate of 3.12 times the rate of Leu-Enk during experimenter handling suggesting a linear relationship between the two peptides. **D.** A negative correlation (-0.3141) shows that if a high concentration of Met-Enk is released in the first two samples, the concentration released in later samples is affected; such influence suggests that there is regulation of the maximum amount of peptide to be released in NAcSh. **E.** The negative correlation in panel d is reversed by using high K+ buffer to evoke Met-Enk release, suggesting that the limited release observed in **D** is due to modulation of peptide release rather than depletion of reserves. Data in **A-E** are transformed to a log scale and n=24 animals. In panel **A**, 2-way ANOVA analysis shows a main effect of peptide, treatment, and interaction. The *p*-values reported were calculated using a Sidak's multiple comparisons test. **F.** Schematic describing the viral strategy and probe placement for the fiber photometry experiment in pEnk-Cre mice injected with the calcium sensor GCaMP6s in the NAcSh. **G.** Average z-score trace following the first, second, and third events involving experimenter handling. **H**. Heatmaps showing individual mouse z-scored fiber photometry responses before and after experimenter handling. **I**. Bar graphs showing the averaged z-score responses before experimenter handling and after experimenter handling (n=10 for **G-I**).

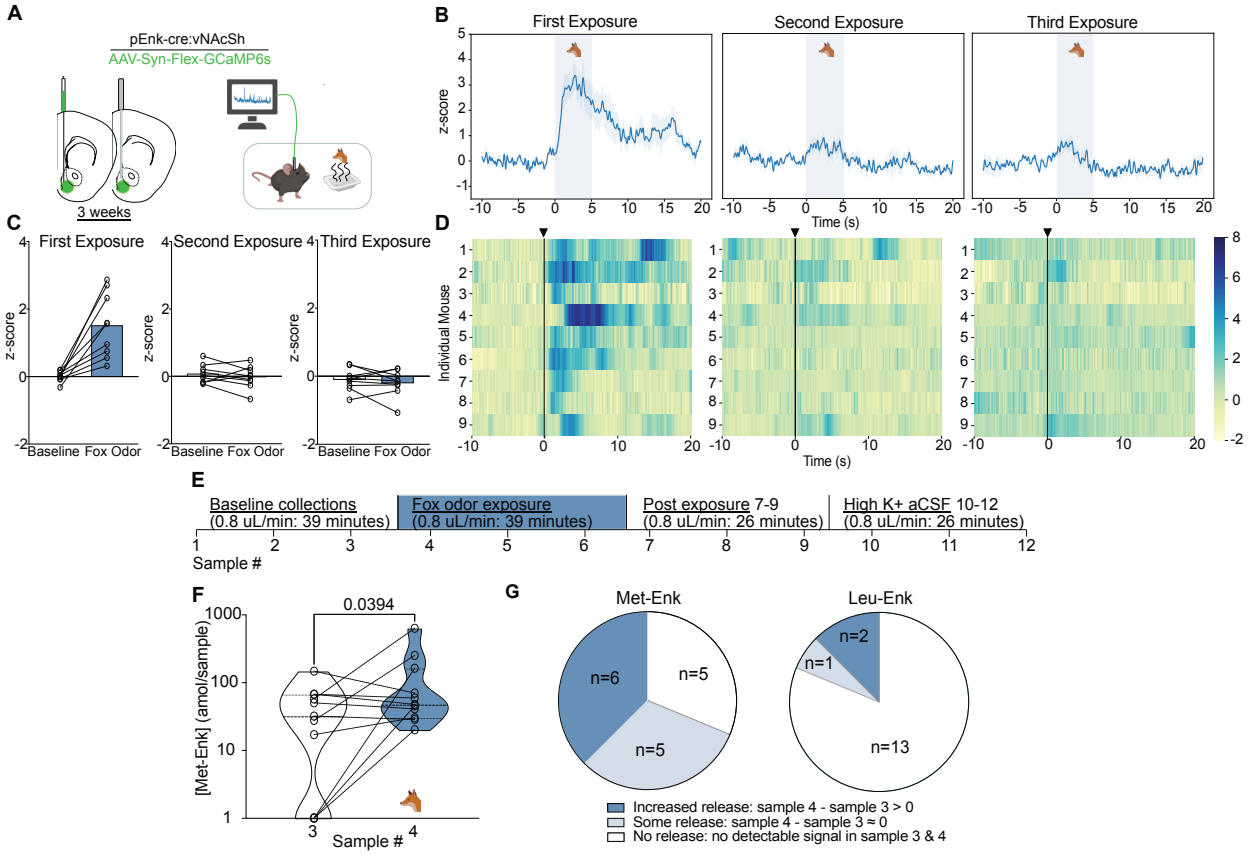
A
pEnk-cre:vNAcSh
AAV-Syn-Flex-GCaMP6s
3 weeks
B
First Exposure
Second Exposure
Third Exposure
z-score
Time (s)
C
First Exposure
Second Exposure
Third Exposure
z-score
Baseline Fox Odor
D
Individual Mouse
Time (s)
E
Baseline collections
(0.8 uL/min: 39 minutes)
Fox odor exposure
(0.8 uL/min: 39 minutes)
Post exposure 7-9
(0.8 uL/min: 26 minutes)
High K+ aCSF 10-12
(0.8 uL/min: 26 minutes)
Sample #
F
0.0394
[Met-Enk] (amol/sample)
Sample #
G
Met-Enk
Leu-Enk
n=6
n=5
n=5
n=2
n=1
n=13
Increased release: sample 4 - sample 3 > 0
Some release: sample 4 - sample 3 ≈ 0
No release: no detectable signal in sample 3 & 4

Figure 3. Fox odor exposure activates enkephalinergic neurons and drives the release of Met-Enk in the NAcSh. A. Viral strategy and probe placement for the fiber photometry experiment in pEnk-Cre mice injected with the calcium sensor GCaMP6s in the NAcSh. **B.** Averaged z-score traces of the first, second, and third exposure to fox odor. **C.** Bar graphs showing the averaged z-scored fiber photometry responses before and after exposure to fox odor **D**. Heatmaps showing individual mouse z-scored fiber photometry responses before and after exposure to fox odor. (n=9, for **A-D**) **E**. Experimental timeline describing the fox odor microdialysis experiment. **F**. There is a significant increase in Met-Enk concentration during fox odor exposure (sample 4), in comparison to sample, 3 before odor exposure. Data is transformed to a log scale and the *p*-value was calculated using a paired t-test (n=11). **G.** Pie charts showing the variation across animals in Met-Enk and Leu-Enk release profiles in response to exposure to fox odor, suggesting that such exposure may selectively cause the release of Met-Enk but not Leu-Enk. Increased release showed higher concentration of Met-Enk during exposure to fox odor (sample 4) than the sample before (sample 3), some release showed a comparable level to the sample before exposure, and no release showed no quantifiable concentration during exposure to fox odor.

358 **Materials and Methods:**

359 **List of Abbreviatons:**

360 FA, formic acid
361 MeCN, acetonitrile
362 MeOH, methanol
363 DIA, Data-Independent Acquisition
364 AGC, Automatic Gain Control
365 *nano*-LC-MS, capillary liquid chromatography interfaced to a mass spectrometer
366 MS1, mass spectra of peptide precursors
367 MS2, fragmentation mass spectrum of peptide from precursor ion
368
369 **Reagents**

370 Acetonitrile (MeCN; J.T. Baker, cat. no. 9829-03)

371 Water (J.T. Baker, cat. no. 4218-03)

372 Formic Acid (FA; Sigma-Aldrich, cat. no. 56302)

373 Hydrogen Peroxide (Fisher Chemical, cat. no. H325-100)

374 Methanol (MeOH; Fluka, cat. no. 34966)

375 **Equipment**

376 Stage tips

377 Laboratory pipetting needles with 90° blunt ends, 16-gauge, 2-inch length; Cadence Science,
378 cat. no. 7938)

379 C18 extraction disks, diam. = 47 mm, 20 pack; (Empore, cat. no. 66883-U)

380 Adapter for stage tipping (Glygen, cat. no. CEN.24)

381 1.5-ml tubes (Axygen, Cat. No. MCT-175-C)
382 Eppendorf centrifuge (Eppendorf, model 5424R)

383 Vortex (Labnet VX100)

384 Autosampler vials (Sun-Sri, Cat. No. 200046)

385 Autosampler vial caps (Sun-Sri, cat. no. 501 382)

386 UPLC system for LC-MS of analysis of TMT-labeled peptides (EASY nL-LC 1000, Thermo
387 Scientific)

388 Mass spectrometer for analysis of TMT-labeled peptides (Q-Exactive™ Plus Hybrid Quadrupole
389 Orbitrap™, Thermo Scientific)

390 EASY-Spray™ column, 75 µm x 50 cm PepMap (Thermo Scientific™, cat. no. ES903)

391

392

393 **Animals**

394 Adult male and female C57BL/6 mice at 8-15 weeks of age were used for microdialysis
395 procedures. For fiber photometry, adult preproEnkephalin-Cre (pEnk-Cre) male and female mice
396 at ages between 15-24 weeks of age were used to measure enkephalinergic cell activity. Mice
397 were group housed and kept at a 12-hour light/dark cycle with *ad libitum* access to water and
398 food. The holding facility was both temperature and humidity controlled. All surgical and
399 behavioral procedures were approved by the Washington University School of Medicine animal
400 care guidelines in accordance with federal animal use regulations.

401 **Chemicals**

402 Met and Leu Enkephalin standards including isotopically labeled forms were synthesized at New
403 England Peptide and can be ordered by the research community. The heavy isotope labeled Leu
404 Enkephalin is synthesized with a fully labeled L-Leucine ($^{13}C_6$, ^{15}N) at the C terminus of the peptide
405 (YGGF**L**). For Met Enkephalin, a fully labeled L-Phenylalanine ($^{13}C_9$, ^{15}N) was added (YGG**F**M).
406 The resulting mass shift between the endogenous (light) and heavy isotope-labeled peptide are
407 7Da and 10Da, respectively. Heavy isotope amino acids are guaranteed >99% pure. Peptide
408 purity specifications are set at ≥ 95% pure by area on a regular HPLC gradient with UV detection.
409 Artificial cerebrospinal fluid (aCSF) contained 124 mM NaCl, 2.5 mM KCl, 2 mM $CaCl_2$, 1 mM
410 $MgCl_2$, 1.25 mM NaH_2PO_4, 24 mM $NaHCO_3$, 5 mM HEPES, 12.5 mM Glucose adjusted to pH 7.4
411 with NaOH. High K^+ ringer solution contained 48 mM NaCl, 100 mM KCl, 2.4 mM $CaCl_2$, 0.85 mM
412 $MgCl_2$ adjusted to pH 7.4 with NaOH as described in (Al-Hasani, 2018). All salt compounds were
413 purchased from Sigma (St. Louis, MO).

414 ***In vivo* microdialysis**

415 Custom microdialysis probes (BASI Inc. part MD-2206) of 5 mm shaft length and 1 mm
416 Polyacrylonitrile membrane with a 30 kDa molecular weight cutoff were used for the *in vivo*
417 experiments. The probes were flushed prior to surgical implantation for 15 minutes at 10 μL/min
418 with artificial cerebrospinal fluid as directed by the manufacturer using a BASI syringe pump (MD

419 1001). For the surgical procedure, mice were briefly anaesthetized in an induction chamber at 3%
420 isofluorane before being placed in a stereotaxic frame (Kopf) secured with ear and bite bars.
421 During the surgery, the isofluorane level was kept at 1.5-2%. The probe was then inserted into
422 the ventral Nucleus Accumbens shell (stereotaxic coordinates from bregma: +1.3 [AP], ±0.5 [ML],
423 −5.0 mm [DV]). Implanted probes were secured with dental adhesive (C&B metabond kit) followed
424 by cyanoacrylate (Loctite superglue gel control).
425 After the completion of the surgery, each mouse was allowed to recover for 30 minutes. The
426 mouse was then connected to an inlet perfusion line to circulate aCSF or high K+ ringer solution
427 and an outlet perfusion line to collect the interstitial fluid from the NAcSh. The outlet line directly
428 collected sample in a tube that is kept at 4 °C throughout the experiment. The flow of aCSF was
429 then then turned on and sample collection time started as sample began to collect in the outlet
430 tube. The flow rate of aCSF was set to 0.8 μL/min during sample collection. Fractions were
431 collected every 13 minutes resulting in a 10 μL sample. After each collection, the samples were
432 spiked with 2 μL of 12.5 fM isotopically labeled Met-Enkephalin and Leu-Enkephalin. The
433 microdialysis rig (BASI Raturn MD 1404) was equipped with bedding, regular mouse chow and
434 water ad libitum. While connected to the perfusion lines, the mice were allowed to move freely.
435 For the experiments measuring evoked release, the high K+ ringer solution was perfused through
436 the lines instead of aCSF at 0.8 μL/min and fractions were collected every 13 minutes as
437 described previously. The samples were similarly spiked with 2 μL of 12.5 fM isotopically labeled
438 Met-Enkephalin and Leu-Enkephalin.
439 For the experiments where the animals were exposed to the fox urine odor, 3 mL of fox urine was
440 absorbed into a kim wipe contained in a chemical weigh boat. The weigh boats were prepared
441 and remained in a fume hood the experiment to prevent the odor permeating the experimental
442 space before the planned collection. Then, the experimenter placed the weigh boat in the
443 microdialysis rig and allowed the mouse to explore it. The exposure was standardized to span 3

444 fractions (39 minutes) during each of the experiments while aCSF was being perfused through
445 the lines.

446 **In vivo sample processing**

447 ***Methionine Oxidation Reaction***

448 For met-enkephalin detection and stabilization, the animal samples underwent a methionine
449 oxidation reaction [21]. To each sample vial, 28 μl of 0.1% (vol/vol) formic acid (FA) was added
450 and then the samples were transferred to 0.5 mL tubes from the collection tubes. Afterwards, 40
451 μl of a mixture of 6% FA (vol/vol) and 6% hydrogen peroxide (vol/vol) was added to each of the
452 sample tubes and mixed and gently spun. The samples were then incubated overnight at room
453 temperature.

454 ***Solid Phase Extraction with C18 stage tips***

455 After the methionine oxidation reaction, a solid phase extraction process was performed using
456 C18 stage tips. Stage tips were conditioned before sample loading. To each of the stage tips, 100
457 μl of methanol is added and then spun for 2 minutes at 2,000 rpm in microcentrifuge tubes. The
458 stage tips were then rinsed with 100 μl of a mixture of 50% acetonitrile (MeCN; (vol/vol)) and 0.1%
459 FA (vol/vol) followed by a 2-minute spin at 2,000 rpm. This was followed by a rinse in 0.1% FA
460 (vol/vol) and a 2-minute spin at 3,000 rpm. The final rinse was done by adding 100 μl of 1% FA
461 (vol/vol) to each of the stage tips. Following the final rinse, the samples were added to the C18
462 stage tips and spun for 10 minutes at 0.8 rpm. After ensuring that the samples passed through
463 the stage tips, the samples were desalted with 0.1% FA (vol/vol) and spun for 1.5 minutes at
464 3,000 rpm twice. After the spins were done, the stage tips were directly placed into autosampler
465 vials to elute the analyte with 60 μl of 50% MeCN, 0.1% FA (vol/vol) using a syringe. Eluates in
466 the autosampler vial were dried in a speedvac, reconstituted in 3 μl 1% FA (vol/vol) and set up on
467 the autosampler for injection on the mass spectrometer.

468 ***Nano*-LC-MS/MS.** The samples in formic acid (1%) were loaded (2.5 µl) onto a 75 µm i.d. × 50
469 cm Acclaim® PepMap 100 C18 RSLC column (Thermo-Fisher Scientific) on an EASY *nano*LC
470 (Thermo Fisher Scientific) at a constant pressure of 700 bar at 100% A (1%FA). Prior to sample
471 loading the column was equilibrated to 100%A for a total of 11 µL at 700 bar pressure. Peptide
472 chromatography was initiated with mobile phase A (1% FA) containing 5%B (100%MeCN, 1%FA)
473 for 1 min, then increased to 20% B over 19 min, to 32% B over 10 min, to 95% B over 1 min and
474 held at 95% B for 19 min, with a flow rate of 250 nL/min. The data was acquired in data-
475 independent acquisition (DIA) mode. The full-scan mass spectra were acquired with the Orbitrap
476 mass analyzer with a scan range of *m/z* = 150 to 1500 and a mass resolving power set to 70,000.
477 Data-independent (DIA) high-energy collisional dissociations were performed according to the
478 inclusion list with a mass resolving power set to 17,500, an isolation width of 2 Da, and a
479 normalized collision energy setting of 27. The maximum injection time was 60 ms for parent-ion
480 analysis and product-ion analysis. The automatic gain control (AGC) was set at a target value of
481 3e6 ions for full MS scans and 2e5 ions for MS2. The inclusion list contained 4 peptide entries.
482 The loop count was set at 30. Retention time windows were set at 20 min.

483 **Stable-isotope dilution assay for measurement of enkephalins**

484 Peptides were synthesized as high purity natural abundance and stable isotope-labeled pairs.
485 Assays were developed as Tier 2 assays according to CPTAC guidelines [22]. Co-eluting peak
486 boundaries for the internal standard and endogenous peptides were manually refined using the
487 Skyline software package [49]. Integrated peak areas for the three most intense fragment ions
488 were then exported for determination of peak area ratios of endogenous to internal standard
489 signal, which were used as a basis for determining abundance and quantifying changes in
490 enkephalin levels in mouse studies.

491 ***In vivo* fiber photometry**
492
493 <u>Stereotaxic surgery</u>

494 For the surgical procedure, pEnk-Cre mice were briefly anaesthetized in an induction chamber at
495 3% isofluorane before being placed in a stereotaxic frame (Kopf) secured with ear and bite bars.
496 During the surgery, the isofluorane level was kept at 1.5-2%. Then we performed a craniotomy
497 and unilaterally injected using a Nanoject III (Drummond) 200-250 nL of
498 AAV5.Syn.Flex.GCaMP6s.WPRE.SV40 (Addgene: 100845-AAV5) at the following coordinates
499 :+1.3 [AP],±0.5 [ML], −5.0 mm [DV]. To allow for viral expression, the fiber photometry probes (5
500 mm shaft length, doric lenses) were implanted 3 weeks later at +1.3 [AP], ±0.5 [ML], −4.75 mm
501 [DV]. Implanted probes were secured with dental adhesive (C&B metabond kit) followed by
502 cyanoacrylate (Loctite superglue gel control).

503 Fiber photometry recording procedure

504 Before recording, the implanted probes were tethered to an optic fiber using a ferrule sleeve
505 (Doric, catalog no. ZR_2.5). Two light-emitting diodes (LEDs) were used to excite GCaMP6s. A
506 331 Hz sinusoidal LED light (Doric) of wavelength 470 nm 470 ± 20 nm was used for the Ca^{2+} -
507 dependent signal. A 210 Hz sinusoidal LED light of wavelength 405 ± 10 nm (Doric, LED driver)
508 was used to evoke the Ca^{2+} -independent signal and serve as the isosbestic control. GCaMP6s
509 fluorescence traveled through the same optic fiber before being bandpass filtered (525 ± 25 nm,
510 Doric, catalog no. FMC4), transduced by a femtowatt photoreceiver (New Focus Model 2151) and
511 recorded by a real-time processor (TDT, RZ5P). The signals were extracted by the Synapse
512 software (TDT). During the recording, two behavioral manipulations were introduced. The first
513 was after a 10-minute recording in a home cage environment, an experimenter handled the
514 mouse while the recording was ongoing. The mouse was then let go and the handling was
515 repeated another two times in a single session. The second behavioral manipulation was
516 introduced to the same mice a week after the first recording session. After a 10-minute recording
517 in the home-cage environment, a weight boat containing a kim wipe that had absorbed 3 mL of
518 fox urine was placed in the cage as the recording proceeded. The weigh boat was removed after

519 a minute of exploration then re-introduced into the cage for another two times, separated by 5
520 minutes from the last exposure, during the session.

521 Fiber Photometry Data Analysis

522 Data analysis was performed through the python toolbox GuPPy [50]. Briefly, the isosbestic
523 control signal was used to correct for motion and photobleaching artifacts. The control channel is
524 fitted to the signal channel using a least squares polynomial fit of degree 1. Transient detection
525 occurred after using a 15s moving window for thresholding transients. Then, high-amplitude
526 events were identified and their timestamp of occurrence during the session was reported. To
527 determine the effect of handling or fox urine exposure on enkephalinergic cell activity, the event
528 timestamp was used to observe changes in activity before and after the behavioral manipulation.
529 The average of all trials is then calculated for repeated exposures and for exposures in multiple
530 animals. The fiber photometry data was represented as z-scores.

531 Immunohistochemistry and verification of probe placement

532 After the completion of the experiment, mice were anaesthetized with a mixture of ketamine,
533 xylazine and acepromazine and transcardially perfused with ice-cold 4% paraformaldehyde in
534 phosphate buffer. After the perfusion, brains were dissected and fixed for 24 hours in 4%
535 paraformaldehyde at 4°C and then placed in 30% sucrose solution for cryoprotection for a
536 minimum of 48 hours. The brains were then sliced into 30 um sections, washed three times in
537 PBS and blocked in PBS containing 0.5% Triton X-100 and 5% goat serum for one hour. Following
538 the blocking step, the slices were stained for the glial fibrillary acidic protein (GFAP), an astrocyte
539 marker to determine glial scarring around the probe site (guinea pig anti-GFAP, synaptic systems)
540 at 1:500 dilution and incubated at 4°C for 16 hours. The next day, the sections were washed three
541 times with PBS and stained with the secondary antibody, mouse anti-guinea pig, Alexa Fluor 594
542 (Invitrogen) at 1:500 dilution and incubated for two hours at room temperature. After the
543 incubation, the slices were washed three times in PBS, followed by two washes with PB. Finally,
544 the slices were mounted on glass slides with Hard set Vectashield with DAPI staining (Vector

545 Labs) and imaged using an epifluorescence microscope (Leica DM6 B). Correct probe placement
546 in the NAcSh is represented in **supplementary figure 1B**.
547 For the verification of the injection and probe placement for fiber photometry, the same procedure
548 described above was performed for tissue preparation. After slicing, the slices were washed in a
549 0.1% Triton for one hour in order to permeabilize the cells followed by two 10-minute PBS washes.
550 The slices were then stained with Neurotrace (Nissl) red (Invitrogen) to mark neurons by adding
551 5 μL to each well for 2 hours at room temperature followed by 3 10-minute PBS washes and 3
552 10-minute PB washes. Finally, the slices were mounted using Hard set Vectashield (Vector Labs).
553 GCaMP6s expression was determined by observing green fluorescent protein expression
554 colocalized with Neurotrace staining. Correct probe placement in the NAcSh is represented in
555 **supplementary figure 1D**.

556 **Statistical Analysis**

557 We performed simple linear regression analysis on the forward and reverse curves and reported
558 the line equations. The proteomics data is represented as violin plots with individual points
559 depicted and dashed lines indicating quartiles. The middle-dashed lines represent the median.
560 The data was log transformed to reduce the skewness of the dataset caused by the variable range
561 of concentrations measured across experiments/animals prior to Two-way ANOVA testing with
562 peptide (Met-Enk or Leu-Enk) and treatment (buffer or stress for example) as the two independent
563 variables. A paired t-test was performed on the predator odor proteomic data before and after
564 treatment. To correlate the levels of Met-Enk to Leu-Enk in the same samples, we conducted
565 simple linear regression analysis and reported the slopes of the lines. For the fiber photometry
566 data, the z-scores were calculated as described in [50]. For the averaged plots, z-scores from all
567 individual animals were averaged and shown as one trace with the SEM as the highlighted area.
568

569 **Funding**

570 This work was supported by National Institutes on Drug Abuse R00 DA038725 (RA) and

R21DA048650 (RA). The NARSAD Young Investigator Grant from the Brain and Behavior Research Foundation, grant no. 28243 (RA). The WU-PSR is supported in part by the WU Institute of Clinical and Translational Sciences (NCATS UL1 TR000448), the Mass Spectrometry Research Resource (NIGMS P41 GM103422; R24GM136766) and the Siteman Comprehensive Cancer Center Support Grant (NCI P30 CA091842). Cognitive, Computational, and Systems Neuroscience Fellowship (MOM).

Author Contributions

- Conceptualization: RA, MOM, RRT, RS
- Methodology: MOM, RA, PEG, RC, JM, RS
- Investigation: MOM, PEG, RC, SMC, JW
- Formal Analysis: MOM, PEG, RS
- Visualization: MOM, JM
- Supervision: RA, RRT, RS
- Writing—original draft: MOM, PEG, RS
- Writing—review & editing: RA, MOM, PEG, RC, SMC, JM, JW, RS, RRT

Acknowledgments

The figure schematics were created with biorender.com. We would like to thank Justin W. Baldwin for his guidance on appropriate data visualization tools and for his support in proofreading the manuscript. We would also like to thank Dr. Jordan McCall for his advice on data analysis and visualization as well as proofreading the manuscript. Thank you to Emily Wheeler for proofreading the manuscript and providing feedback on sentence structure and flow. We would also like to thank the entirety of the proteomics core team including Dr. Yiling Mi for her assistance. Thank you to the entirety of the Al-Hasani and McCall labs for their feedback on experimental design and analysis. Finally, thank you to Dr. Tim Holy, Dr. Robyn Klein, and Dr. Alexxai Kravitz for their feedback.

596

597

598

References

[1] L.D. Fricker, E.B. Margolis, I. Gomes, L.A. Devi, Five Decades of Research on Opioid Peptides: Current Knowledge and Unanswered Questions, Mol Pharmacol. 98 (2020) 96–108. https://doi.org/10.1124/MOL.120.119388.

[2] M.R. Banghart, X.J. He, B.L. Sabatini, A Caged Enkephalin Optimized for Simultaneously Probing Mu and Delta Opioid Receptors, ACS Chem Neurosci. 9 (2018) 684–690. https://doi.org/10.1021/ACSCHEMNEURO.7B00485/ASSET/IMAGES/LARGE/CN-2017-00485A_0003.JPEG.

[3] I. Gomes, S. Sierra, L. Lueptow, A. Gupta, S. Gouty, E.B. Margolis, B.M. Cox, L.A. Devi, Biased signaling by endogenous opioid peptides, Proceedings of the National Academy of Sciences. 117 (2020) 11820–11828. https://doi.org/10.1073/pnas.2000712117.

[4] A. Mansour, M.T. Hoversten, L.P. Taylor, S.J. Watson, H. Akil, The cloned μ, δ and κ receptors and their endogenous ligands: Evidence for two opioid peptide recognition cores, Brain Res. 700 (1995) 89–98. https://doi.org/10.1016/0006-8993(95)00928-J.

[5] M.R. Banghart, S.Q. Neufeld, N.C. Wong, B.L. Sabatini, Enkephalin Disinhibits Mu Opioid Receptor-Rich Striatal Patches via Delta Opioid Receptors, Neuron. 88 (2015) 1227–1239. https://doi.org/10.1016/J.NEURON.2015.11.010.

[6] N.T. Maidment, D.R. Brumbaugh, V.D. Rudolph, E. Erdelyi, C.J. Evans, Microdialysis of extracellular endogenous opioid peptides from rat brain in vivo, Neuroscience. 33 (1989) 549–557. https://doi.org/10.1016/0306-4522(89)90407-7.

[7] P.W. Marinelli, L. Bai, R. Quirion, C. Gianoulakis, A Microdialysis Profile of Met-Enkephalin Release in the Rat Nucleus Accumbens Following Alcohol Administration, Alcohol Clin Exp Res. 29 (2005) 1821–1828. https://doi.org/10.1097/01.alc.0000183008.62955.2e.

[8] L. Hemandez, B.G. Hoebel, Food reward and cocaine increase extracellular dopamine in the nucleus accumbens as measured by microdialysis, 1988.

[9] M.M. Nieto, J. Wilson, A. Cupo, B.P. Roques, F. Noble, Chronic Morphine Treatment Modulates the Extracellular Levels of Endogenous Enkephalins in Rat Brain Structures Involved in Opiate Dependence: A Microdialysis Study, The Journal of Neuroscience. 22 (2002) 1034–1041. https://doi.org/10.1523/JNEUROSCI.22-03-01034.2002.

[10] O.S. Mabrouk, Q. Li, P. Song, R.T. Kennedy, Microdialysis and Mass Spectrometric Monitoring of Dopamine and Enkephalins in the Globus Pallidus Reveal Reciprocal Interactions that Regulate Movement, J Neurochem. 118 (2011) 24. https://doi.org/10.1111/J.1471-4159.2011.07293.X.

[11] Q. Li, Jon-Kar Zubieta, R.T. Kennedy, Practical Aspects of in Vivo Detection of Neuropeptides by Microdialysis Coupled Off-Line to Capillary LC with Multi-stage MS, Anal Chem. 81 (2009) 2242. https://doi.org/10.1021/AC802391B.

[12] H.M. Baseski, C.J. Watson, N.A. Cellar, J.G. Shackman, R.T. Kennedy, Capillary liquid chromatography with MS3 for the determination of enkephalins in microdialysis samples from the striatum of anesthetized and freely-moving rats, Journal of Mass Spectrometry. 40 (2005) 146–153. https://doi.org/10.1002/jms.733.

[13] R. Al-Hasani, J.-M.T. Wong, O.S. Mabrouk, J.G. McCall, G.P. Schmitz, K.A. Porter-Stransky, B.J. Aragona, R.T. Kennedy, M.R. Bruchas, In vivo detection of optically-evoked opioid peptide release, Elife. 7 (2018). https://doi.org/10.7554/eLife.36520.

[14] R. Al-Hasani, J.G. McCall, G. Shin, A.M. Gomez, G.P. Schmitz, J.M. Bernardi, C.-O. Pyo, S. il Park, C.M. Marcinkiewcz, N.A. Crowley, M.J. Krashes, B.B. Lowell, T.L. Kash, J.A. Rogers, M.R. Bruchas, Distinct Subpopulations of Nucleus Accumbens Dynorphin Neurons Drive Aversion and Reward., Neuron. 87 (2015) 1063–77. https://doi.org/10.1016/j.neuron.2015.08.019.

[15] B.E. Pirino, M.B. Spodnick, A.T. Gargiulo, G.R. Curtis, J.R. Barson, A.N. Karkhanis, Kappa-opioid receptor-dependent changes in dopamine and anxiety-like or approach-

avoidance behavior occur differentially across the nucleus accumbens shell rostro-caudal axis, Neuropharmacology. 181 (2020). https://doi.org/10.1016/J.NEUROPHARM.2020.108341.

[16] B.H. Trieu, B.C. Remmers, C. Toddes, D.D. Brandner, E.M. Lefevre, A. Kocharian, C.L. Retzlaff, R.M. Dick, M.A. Mashal, E.A. Gauthier, W. Xie, Y. Zhang, S.S. More, P.E. Rothwell, Angiotensin-converting enzyme gates brain circuit–specific plasticity via an endogenous opioid, Science (1979). 375 (2022) 1177–1182. https://doi.org/10.1126/SCIENCE.ABL5130/SUPPL_FILE/SCIENCE.ABL5130_DATA_S1.ZIP.

[17] S.M. Reynolds, K.C. Berridge, Positive and negative motivation in nucleus accumbens shell: bivalent rostrocaudal gradients for GABA-elicited eating, taste “liking”/"disliking" reactions, place preference/avoidance, and fear, J Neurosci. 22 (2002) 7308–7320. https://doi.org/10.1523/JNEUROSCI.22-16-07308.2002.

[18] D.C. Castro, M.R. Bruchas, A Motivational and Neuropeptidergic Hub: Anatomical and Functional Diversity within the Nucleus Accumbens Shell, Neuron. 102 (2019) 529–552. https://doi.org/10.1016/J.NEURON.2019.03.003.

[19] A.G. Schindler, D.I. Messinger, J.S. Smith, H. Shankar, R.M. Gustin, S.S. Schattauer, J.C. Lemos, N.W. Chavkin, C.E. Hagan, J.F. Neumaier, C. Chavkin, Stress produces aversion and potentiates cocaine reward by releasing endogenous dynorphins in the ventral striatum to locally stimulate serotonin reuptake, J Neurosci. 32 (2012) 17582–17596. https://doi.org/10.1523/JNEUROSCI.3220-12.2012.

[20] D.C. Castro, K.C. Berridge, Opioid Hedonic Hotspot in Nucleus Accumbens Shell: Mu, Delta, and Kappa Maps for Enhancement of Sweetness “Liking” and “Wanting,” Journal of Neuroscience. 34 (2014) 4239–4250. https://doi.org/10.1523/JNEUROSCI.4458-13.2014.

[21] J.J. Pesavento, B.A. Garcia, J.A. Streeky, N.L. Kelleher, C.A. Mizzen, Mild performic acid oxidation enhances chromatographic and top down mass spectrometric analyses of histones, Mol Cell Proteomics. 6 (2007) 1510–1526. https://doi.org/10.1074/MCP.M600404-MCP200.

[22] S.A. Carr, S.E. Abbatiello, B.L. Ackermann, C. Borchers, B. Domon, E.W. Deutsch, R.P. Grant, A.N. Hoofnagle, R. Hüttenhain, J.M. Koomen, D.C. Liebler, T. Liu, B. MacLean, D.R. Mani, E. Mansfield, H. Neubert, A.G. Paulovich, L. Reiter, O. Vitek, R. Aebersold, L. Anderson, R. Bethem, J. Blonder, E. Boja, J. Botelho, M. Boyne, R.A. Bradshaw, A.L. Burlingame, D. Chan, H. Keshishian, E. Kuhn, C. Kinsinger, J.S.H. Lee, S.W. Lee, R. Moritz, J. Oses-Prieto, N. Rifai, J. Ritchie, H. Rodriguez, P.R. Srinivas, R.R. Townsend, J. van Eyk, G. Whiteley, A. Wiita, S. Weintraub, Targeted peptide measurements in biology and medicine: Best practices for mass spectrometry-based assay development using a fit-for-purpose approach, Molecular and Cellular Proteomics. 13 (2014) 907–917. https://doi.org/10.1074/MCP.M113.036095/ATTACHMENT/D53FF2E2-A6B1-4AAD-BC0D-B7F9E6821120/MMC1.PDF.

[23] A.G. Difeliceantonio, O.S. Mabrouk, R.T. Kennedy, K.C. Berridge, Enkephalin surges in dorsal neostriatum as a signal to eat, Current Biology. 22 (2012) 1918–1924. https://doi.org/10.1016/J.CUB.2012.08.014.

[24] T.L. Ripley, J. Jaworski, P.K. Randall, R.A. Gonzales, Repeated perfusion with elevated potassium in in vivo microdialysis - A method for detecting small changes in extracellular dopamine, J Neurosci Methods. 78 (1997) 7–14. https://doi.org/10.1016/S0165-0270(97)00129-5.

[25] M. Comb, P.H. Seeburg, J. Adelman, L. Eiden, E. Herbert, Primary structure of the human Met- And Leu-enkephalin precursor and its mRNA, Nature. 295 (1982) 663–666. https://doi.org/10.1038/295663a0.

[26] J. HUGHES, H.W. KOSTERLITZ, T.W. SMITH, THE DISTRIBUTION OF METHIONINE-ENKEPHALIN AND LEUCINE-ENKEPHALIN IN THE BRAIN AND PERIPHERAL TISSUES, Br J Pharmacol. 120 (1997) 428–436. https://doi.org/10.1111/j.1476-5381.1997.tb06829.x.
[27] G. Henderson, J. Hughes, H.W. Kosterlitz, In vitro release of Leu- and Met-enkephalin from the corpus striatum, Nature 1978 271:5646. 271 (1978) 677–679. https://doi.org/10.1038/271677a0.
[28] T. Yoshimasa, K. Nakao, H. Ohtsuki, S. Li, H. Imura, Methionine-enkephalin and leucine-enkephalin in human sympathoadrenal system and pheochromocytoma, Journal of Clinical Investigation. 69 (1982) 643–650. https://doi.org/10.1172/JCI110491.
[29] J.A. Mansi, S. Laforest, G. Drolet, Effect of stress exposure on the activation pattern of enkephalin-containing perikarya in the rat ventral medulla, J Neurochem. 74 (2000) 2568–2575. https://doi.org/10.1046/J.1471-4159.2000.0742568.X.
[30] E.C. Dumont, R. Kinkead, J.F. Trottier, I. Gosselin, G. Drolet, Effect of chronic psychogenic stress exposure on enkephalin neuronal activity and expression in the rat hypothalamic paraventricular nucleus, J Neurochem. 75 (2000) 2200–2211. https://doi.org/10.1046/J.1471-4159.2000.0752200.X.
[31] S. Ceccatelli, C. Orazzo, Effect of different types of stressors on peptide messenger ribonucleic acids in the hypothalamic paraventricular nucleus, Acta Endocrinol (Copenh). 128 (1993) 485–492. https://doi.org/10.1530/ACTA.0.1280485.
[32] R.J. Valentino, E. van Bockstaele, Endogenous opioids: The downside of opposing stress, Neurobiol Stress. 1 (2015) 23–32. https://doi.org/10.1016/J.YNSTR.2014.09.006.
[33] H. Nam, R. Chandra, T.C. Francis, C. Dias, J.F. Cheer, M.K. Lobo, Reduced nucleus accumbens enkephalins underlie vulnerability to social defeat stress, Neuropsychopharmacology. 44 (2019) 1876–1885. https://doi.org/10.1038/s41386-019-0422-8.
[34] J.W. de Jong, S.A. Afjei, I. Pollak Dorocic, J.R. Peck, C. Liu, C.K. Kim, L. Tian, K. Deisseroth, S. Lammel, A Neural Circuit Mechanism for Encoding Aversive Stimuli in the Mesolimbic Dopamine System, Neuron. 101 (2019) 133-151.e7. https://doi.org/10.1016/J.NEURON.2018.11.005.
[35] R. Apfelbach, C.D. Blanchard, R.J. Blanchard, R.A. Hayes, I.S. McGregor, The effects of predator odors in mammalian prey species: A review of field and laboratory studies, Neurosci Biobehav Rev. 29 (2005) 1123–1144. https://doi.org/10.1016/J.NEUBIOREV.2005.05.005.
[36] T. Endres, M. Fendt, Aversion- Vs fear-inducing properties of 2,4,5-trimethyl-3-thiazoline, a component of fox odor, in comparison with those of butyric acid, Journal of Experimental Biology. 212 (2009) 2324–2327. https://doi.org/10.1242/jeb.028498.
[37] V. Farmer-Dougan, S. Chandrashekar, D. Stutzman, K. Bradham, J.D. Dougan, Fox urine as an aversive stimulus: modification of a passive avoidance task, J Gen Psychol. 132 (2005) 313–320. https://doi.org/10.3200/GENP.132.3.313-320.
[38] A.L.O. Hebb, R.M. Zacharko, M. Gauthier, F. Trudel, S. Laforest, G. Drolet, Brief exposure to predator odor and resultant anxiety enhances mesocorticolimbic activity and enkephalin expression in CD-1 mice, European Journal of Neuroscience. 20 (2004) 2415–2429. https://doi.org/10.1111/j.1460-9568.2004.03704.x.
[39] A. Asok, L.W. Ayers, B. Awoyemi, J. Schulkin, J.B. Rosen, Immediate early gene and neuropeptide expression following exposure to the predator odor 2,5-dihydro-2,4,5-trimethylthiazoline (TMT), Behavioural Brain Research. 248 (2013) 85–93. https://doi.org/10.1016/J.BBR.2013.03.047.
[40] A.A. Legaria, B.A. Matikainen-Ankney, B. Yang, B. Ahanonu, J.A. Licholai, J.G. Parker, A. v. Kravitz, Fiber photometry in striatum reflects primarily nonsomatic changes in

calcium, Nature Neuroscience 2022 25:9. 25 (2022) 1124–1128. https://doi.org/10.1038/s41593-022-01152-z.

[41] P. Bérubé, J.F. Poulin, S. Laforest, G. Drolet, Enkephalin Knockdown in the Basolateral Amygdala Reproduces Vulnerable Anxiety-Like Responses to Chronic Unpredictable Stress, Neuropsychopharmacology 2014 39:5. 39 (2013) 1159–1168. https://doi.org/10.1038/npp.2013.316.

[42] P. Bérubé, S. Laforest, S. Bhatnagar, G. Drolet, Enkephalin and dynorphin mRNA expression are associated with resilience or vulnerability to chronic social defeat stress, Physiol Behav. 122 (2013) 237–245. https://doi.org/10.1016/J.PHYSBEH.2013.04.009.

[43] I. Melo, E. Drews, A. Zimmer, A. Bilkei-Gorzo, Enkephalin knockout male mice are resistant to chronic mild stress, Genes Brain Behav. 13 (2014) 550–558. https://doi.org/10.1111/GBB.12139.

[44] H.K. Al-Hakeim, S. Zeki Al-Fadhel, A.H. Al-Dujaili, M. Maes, In major depression, increased kappa and mu opioid receptor levels are associated with immune activation, Acta Neuropsychiatr. 32 (2020) 99–108. https://doi.org/10.1017/NEU.2019.47.

[45] Plasma met-enkephalin, beta-endorphin and leu-enkephalin levels in human hepatic encephalopathy, (n.d.). https://apps.who.int/iris/handle/10665/117248 (accessed May 10, 2023).

[46] A.L.O. Hebb, R.M. Zacharko, M. Gauthier, F. Trudel, S. Laforest, G. Drolet, Brief exposure to predator odor and resultant anxiety enhances mesocorticolimbic activity and enkephalin expression in CD-1 mice, European Journal of Neuroscience. 20 (2004) 2415–2429. https://doi.org/10.1111/j.1460-9568.2004.03704.x.

[47] H. Sundberg, K. Døving, S. Novikov, H. Ursin, A method for studying responses and habituation to odors in rats, Behav Neural Biol. 34 (1982) 113–119. https://doi.org/10.1016/S0163-1047(82)91501-1.

[48] A.D. Abraham, S.M. Casello, S.S. Schattauer, B.A. Wong, G.O. Mizuno, K. Mahe, L. Tian, B.B. Land, C. Chavkin, Release of endogenous dynorphin opioids in the prefrontal cortex disrupts cognition, Neuropsychopharmacology 2021. (2021) 1–10. https://doi.org/10.1038/s41386-021-01168-2.

[49] B. MacLean, D.M. Tomazela, N. Shulman, M. Chambers, G.L. Finney, B. Frewen, R. Kern, D.L. Tabb, D.C. Liebler, M.J. MacCoss, Skyline: an open source document editor for creating and analyzing targeted proteomics experiments, Bioinformatics. 26 (2010) 966–968. https://doi.org/10.1093/BIOINFORMATICS/BTQ054.

[50] V.N. Sherathiya, M.D. Schaid, J.L. Seiler, G.C. Lopez, T.N. Lerner, GuPPy, a Python toolbox for the analysis of fiber photometry data, Scientific Reports 2021 11:1. 11 (2021) 1–9. https://doi.org/10.1038/s41598-021-03626-9.